

Zinc Chelation by a Small-Molecule Adjuvant Potentiates Meropenem Activity in Vivo against NDM-1-Producing *Klebsiella pneumoniae*

Shannon B. Falconer,[†] Sarah A. Reid-Yu,[†] Andrew M. King,[†] Sebastian S. Gehrke,[†] Wenliang Wang,[†] James F. Britten,[‡] Brian K. Coombes,[†] Gerard D. Wright,[†] and Eric D. Brown^{*,†}

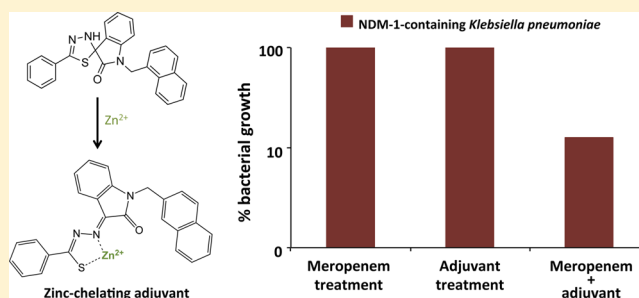
[†]M. G. DeGroot Institute for Infectious Disease Research and Department of Biochemistry and Biomedical Sciences, McMaster University, Hamilton, Ontario L8N 3Z5, Canada

[‡]Department of Chemistry, McMaster University, Hamilton, Ontario L8S 4M1, Canada

Supporting Information

ABSTRACT: The widespread emergence of antibiotic drug resistance has resulted in a worldwide healthcare crisis. In particular, the extensive use of β -lactams, a highly effective class of antibiotics, has been a driver for pervasive β -lactam resistance. Among the most important resistance determinants are the metallo- β -lactamases (MBL), which are zinc-requiring enzymes that inactivate nearly all classes of β -lactams, including the last-resort carbapenem antibiotics. The urgent need for new compounds targeting MBL resistance mechanisms has been widely acknowledged; however, the development of certain types of compounds—namely metal chelators—is actively avoided due to host toxicity concerns. The work herein reports the identification of a series of zinc-selective spiroindoline-thiadiazole analogues that, in vitro, potentiate β -lactam antibiotics against an MBL-carrying pathogen by withholding zinc availability. This study demonstrates the ability of one such analogue to inhibit NDM-1 in vitro and, using a mouse model of infection, shows that combination treatment of the respective analogue with meropenem results in a significant decrease in bacterial burden in contrast to animals that received antibiotic treatment alone. These results support the therapeutic potential of these chelators in overcoming antibiotic resistance.

KEYWORDS: antibiotic adjuvant/ β -lactam resistance/*Klebsiella pneumoniae*/zinc chelator



The ability to effectively treat bacterial infections is indispensable to modern medicine and human health; yet widespread drug resistance mechanisms harbored within bacteria have blunted the efficacy of antibiotics, creating a looming health crisis. The β -lactams are a large class of antibiotics that, despite decades of use, continue to be a mainstay for treating infections caused by Gram-negative bacteria. However, when employed against pathogens that have acquired the ability to produce β -lactamase enzymes, the efficacy of β -lactam antibiotics is severely compromised. Among the most worrisome resistance determinants are the metallo- β -lactamases (MBLs)—a mechanistically distinct class of β -lactamase that employs an active site zinc atom to help catalyze the hydrolysis of the β -lactam ring.¹ Although MBL-producing organisms have not been shown to be intrinsically more virulent than non-MBL-producing pathogens, the concern regarding the former is their recalcitrance to the carbapenem-class β -lactam antibiotics.² Carbapenems are the most recent β -lactam to be developed against a broad range of Gram-negative pathogens and have been invaluable as a last-resort antibiotic to remedy otherwise untreatable infections.^{1,3} Nevertheless, MBL-producing pathogens are increasingly compromising the efficacy

of carbapenems. In addition to their insusceptibility to the action of carbapenems, these organisms tend to harbor multiple drug-resistance determinants, wherein insensitivity to aminoglycosides and quinolones is common.⁴ Thus, for individuals infected with an MBL-producing pathogen, treatment options are extremely limited and the use of antibiotics with significant toxicity, such as colistin, is increasing.⁵ Furthermore, because dissemination of MBL genes occurs via mobile genetic elements, the spread of such resistance enzymes is rapid, as illustrated by the recent emergence—and now global health threat—of the MBL NDM-1.^{1,6}

Antibiotic monotherapies are the traditional course of treatment for bacterial infection; however, the use of drug combinations is not unprecedented.⁷ Such combinations might include two antibiotics that when co-administered result in a synergistic interaction, or a nonantibiotic combined with an antibiotic, with the former acting as an adjuvant to potentiate

Special Issue: Gram-Negative Resistance

Received: March 10, 2015

Published: May 8, 2015

the activity of the latter. The success of adjuvant therapy is exemplified by the clinical use of Zosyn and Augmentin—antibacterial compound combinations that are composed of a β -lactam antibiotic (piperacillin and amoxicillin, respectively) and a β -lactamase inhibitor (tazobactam and clavulanic acid, respectively). Whereas the majority of β -lactamase class enzymes are susceptible to β -lactamase inhibitors, the unique catalytic mechanism of MBLs render these enzymes insensitive to such compounds.⁸

Inhibitors of MBLs represent a serious unmet clinical need that is exacerbated by the significant challenge of identifying compounds that target this class of enzymes. Furthermore, of those molecules that have activity against MBLs in vitro, there is little published research describing in vivo results.⁶ A notable exception is that reported by King et al., where the fungal natural product, aspergillomarasmine A (AMA), was shown to potentiate the action of meropenem against an NDM-1-producing isolate of *Klebsiella pneumoniae* in an animal infection model.⁹ Anti-MBL activity of AMA was shown to occur via zinc removal from the MBL active site. Indeed, the mechanism of zinc binding and metal sequestration by the compound suggests that metal chelation may be a viable route to the potentiation of β -lactam antibiotics in MBL-producing pathogens.

Examples of chelators in clinical use are limited and are generally reserved for disease states that require bulk metal removal from the body, such as iron and copper overload, and heavy metal toxicity.¹⁰ However, there is increasing research toward the potential applications of chelators for medicinal purposes that do not conform to their conventional use as metal detoxifiers. In particular, the development of selective chelators for the treatment of cancer¹¹ and disease states associated with metalloenzymes,¹² as well as various neurodegenerative diseases,¹³ is under active investigation. We speculated that identification of a zinc chelator may have therapeutic potential as an antibiotic adjuvant. Specifically, we reasoned that limiting zinc availability in the bacterial cell should compromise the activity of zinc-dependent metallo- β -lactamases, rendering the bacterium susceptible to β -lactam antibiotics.

We recently reported the discovery of two related spiro-indoline-thiadiazole divalent transition metal chelators that were toxic to bacteria through a mechanism of intracellular iron chelation.¹⁴ Although the antibacterial activity of these chelators could be suppressed with excess iron, we found that addition of the high-affinity iron siderophore enterobactin was sufficient to reverse the activity of these compounds in growth media depleted for transition metals. Furthermore, despite their iron selectivity within bacterial cells, these compounds also showed affinity in vitro to a series of divalent transition metals, including zinc. In the work reported here, we sought to further investigate the potential for developing zinc specificity in the bacterial cell through systematic structural modification of these spiro-indoline-thiadiazole leads. That goal was realized with a series of spiro-indoline-thiadiazole metal chelators that selectively perturb zinc homeostasis in a laboratory strain of *Escherichia coli*. Furthermore, we tested a representative zinc-specific analogue in an animal infection model and showed that the compound was able to resensitize an NDM-1-producing clinical isolate of *K. pneumoniae* to the action of meropenem, without overt toxicity on the host.

RESULTS

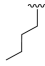
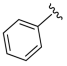
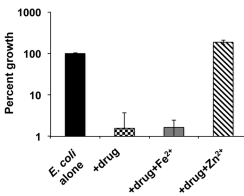
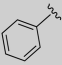
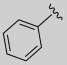
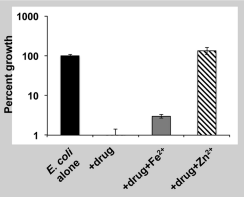
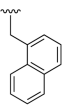
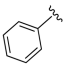
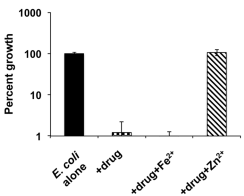
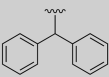
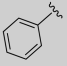
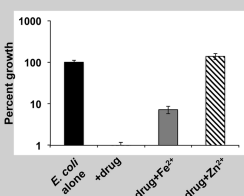
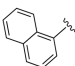
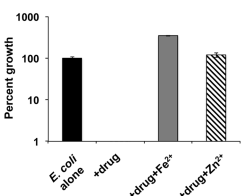
Identification of a Compound Series That Perturbs Zinc Homeostasis in *E. coli* K-12. Motivated by our recent discovery of two spiro-indoline-thiadiazole analogues (SIT-1 and SIT-2) that bound various transition metals, yet selectively perturbed iron homeostasis in *E. coli*, we assembled a series of antibacterial spiro-indoline-thiadiazole analogues to investigate their potential for zinc selectivity (Table 1). We sought to identify small-molecule analogues that, rather than iron, preferentially bind and disrupt the cellular equilibrium of zinc. Our rationale to identify zinc-specific perturbants by exploring spiro-indoline-thiadiazole analogues was based on the hypothesis that chemical modifications to a known transition metal chelator may result in a molecule that, within the complex environment of a bacterial cell, favors zinc rather than iron chelation. Iron and zinc are the most abundant transition metals in bacteria, where *E. coli* has been shown to accumulate concentrations of these metals in the range of 10^{-4} M.^{15,16} Our previous study revealed that antibacterial activity of the chelators SIT-1 and SIT-2 could be suppressed by adding exogenous zinc or iron to metal-depleted media. Nevertheless, we found that the high-affinity iron siderophore enterobactin was sufficient to reverse the activity, leading to the conclusion that the compounds were selective perturbants of iron homeostasis in cells. In these follow-up studies, we reasoned that if exogenous zinc, but not iron, could suppress the lethal phenotype of a given analogue, then perturbation of zinc homeostasis could be considered a possible mechanism of bacterial growth inhibition. We tested 11 spiro-indoline-thiadiazole analogues that were active against *E. coli* K-12 under transition metal-depleted conditions and showed that five of those analogues bore activity that could be suppressed by either ferrous chloride or zinc chloride, where toxicity of the remaining six analogues showed selective suppression by zinc chloride (Table 1). As previously shown, the presence of the sulfur moiety within the diazole backbone was required for both metal chelation and antibacterial activity;¹⁴ hence, all analogues retained this structural core. Analogues of the spiro-indoline-thiadiazole backbone were chosen on the basis of (1) the availability of commercial analogues and (2) the ease and yield of chemical synthesis, which favored modifications at the R1 rather than R2 and R3 positions.

Having observed that the iron perturbants SIT-1 and SIT-2 could be suppressed with the addition of either iron or zinc, we investigated the activity of the phenyl-spiro-indoline-thiadiazole skeleton alone (SIT-3) and found likewise. As compound SIT-1 possesses substituents at both the R1 and R3 positions, we sought to investigate the metal suppression profiles for analogues with a single modification at either the R1 or R3 carbon. Suppression of antibacterial activity by both iron and zinc was retained in the absence of a methyl group at R1 and the presence of a bromide atom at R3 (SIT-4). Compound SIT-Z1, which retained the R1 methyl group yet lacked the R3 bromide, showed a zinc-specific suppression profile. The respective zinc-specific suppression of the antibacterial activity of SIT-Z1 prompted us to explore additional substitutions at the R1 position. In particular, analogues SIT-Z2, SIT-Z3, SIT-Z4, SIT-Z5, and SIT-Z6 possessed various substitutions at the R1 position, and all showed zinc-specific suppression of antibacterial activity. Given that the additions at the R1 position of the Z-series of analogues are carbon-based moieties, we sought to determine whether increasing the overall compound lipophilicity,

Table 1. Structure–Activity Relationship between Spiro-Indoline-Thiadiazole Analogues and Their Antibacterial Activity Metal Suppression Profiles^a

Compound	LogP	MIC (μM)	R ₁	R ₂	R ₃	FeCl ₂ and ZnCl ₂ suppression profiles in <i>E. coli</i>
SIT-1	4.15	16				
SIT-2	4.47	16	H			
SIT-3	3.52	32	H		H	
SIT-4	4.29	16	H			
SIT-Z1	3.38	32			H	
SIT-Z2	3.74	32			H	

Table 1. continued

Compound	LogP	MIC (μM)	R ₁	R ₂	R ₃	FeCl ₂ and ZnCl ₂ suppression profiles in <i>E. coli</i>
SIT-Z3	4.70	16			H	
SIT-Z4	5.04	8			H	
SIT-Z5	6.09	4			H	
SIT-Z6	6.89	4			H	
SIT-5	4.51	16	H		H	

^aBlack bars indicate growth of *E. coli* alone; checkerboard bars show growth of *E. coli* in the presence of an inhibitory concentration of drug; gray bars indicate growth of *E. coli* in the presence of both an inhibitory concentration of drug and an equimolar concentration of ferrous chloride; and hashed bars reveal growth of *E. coli* in the presence of both an inhibitory concentration of drug and an equimolar concentration of zinc chloride.

rather than substitutions specifically at the R₁ position, contributed to the observed compound suppression profiles. Substitution of the R₂ benzyl ring with a naphthyl moiety increased the log *P* from 3.52 (SIT-3) to 4.51 (SIT-5) but imparted no metal specificity to the suppression of antibacterial activity. Thus, substitution at the R₁ position alone appeared to confer zinc-specific suppression.

***E. coli* Toxicity by Z5 Occurs Specifically via Chelation and Perturbation of Zinc Homeostasis.** Our observation that the antibacterial activity of the Z-series of analogues could be suppressed by zinc, but not iron, prompted us to ask whether (1) the Z-series of compounds were capable of chelating both zinc and iron and (2) if chelation does occur, whether the

Z-series exhibit a ligand–metal stoichiometry or denticity that is unique between iron and zinc. We showed via crystal structure determination that, like the known iron perturbant and metal chelator, SIT-1,¹⁴ the merocyanine isomer of SIT-Z5 also chelates ferrous iron with a 2:1 ligand/metal stoichiometry and in a tridentate fashion (Figure S1). In contrast, however, although a crystal structure of SIT-Z5 with zinc also revealed a 2:1 ligand/metal stoichiometry, the denticity was bidentate rather than tridentate (Figure 1). Specifically, the conspicuous difference between the ligand–metal crystal structures of SIT-1–Fe²⁺, SIT-Z5–Fe²⁺, and SIT-Z5–Zn²⁺ was that, in the case of the latter, only atoms N(1'A) and S(1'A)—but not O(1A)—were shown to reside in close enough proximity to the

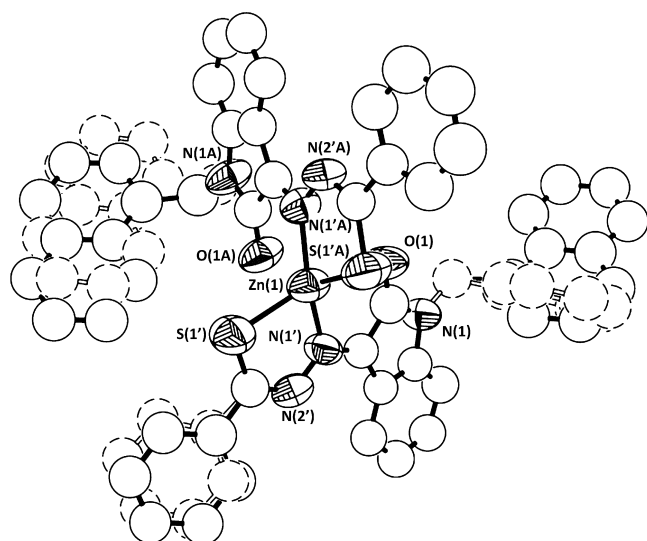


Figure 1. Single crystal structure of SIT-ZS–Zn²⁺ coordination complex. Ellipsoids are at 50% probability. Unlabeled atoms represent carbon, and hydrogen atoms are not shown. The naphthalene moieties and one phenyl group adopted two possible orientations in the crystal, represented here by disorder (dashed lines).

metal to form coordination bonds, indicating a tetrahedral rather than octahedral coordination geometry. With the benefit of a costructure for SIT-ZS with zinc, and given that the ZS analogue was the most potent of the series, we chose to focus on this compound as the representative ligand to understand the antibacterial mechanism of the Z-series of chelators.

Although we determined the capability of SIT-ZS to form a coordination complex with zinc, whether the chelator had another biological effect on the bacterial cell remained unclear. To aid us in answering this question, we used a subinhibitory concentration of compound and screened it against a genomic promoter–reporter collection composed of approximately 2000 bacterial strains, each of which harbored a plasmid containing one of ~2000 different *E. coli* K-12 promoters fused to the green fluorescent protein gene (*gfp*)¹⁷ (Figure 2). This collection enables dynamic, real-time monitoring of promoter activity on perturbation with, for example, a bioactive chemical. In performing this experiment we hypothesized that we would be able to detect any bacterial processes affected by the presence of SIT-ZS via induction of promoter activity and, in turn, fluorescence production. Interestingly, we found that only two promoter *gfp*-containing strains resulted in an increase in fluorescence activity: we observed 5- and 8-fold inductions of promoter activity for the promoters driving expression of the *znuA* and *ykgM* genes, respectively. ZnuA is a component of the *E. coli* high-affinity zinc uptake system that has been shown to be activated under zinc-depleted conditions.¹⁸ YkgM is a paralogue of the ribosomal protein, RpmE, that has lost the zinc-binding motif displayed by the latter protein¹⁹ and which has been shown to undergo increased expression under conditions of zinc limitation.^{20,21} It has been proposed that YkgM replaces the function of RpmE under zinc-depleted conditions. The selective activation of these zinc-dependent promoters suggested that the mechanism of toxicity of SIT-ZS against *E. coli* was indeed due to a specific ability to chelate and perturb zinc homeostasis.

Zinc-Specific Suppression of Compound Activity Correlates with Analogue-Induced Fluorescence of *ykgM* and *znuA* Promoter *gfp* Strains. To confirm that

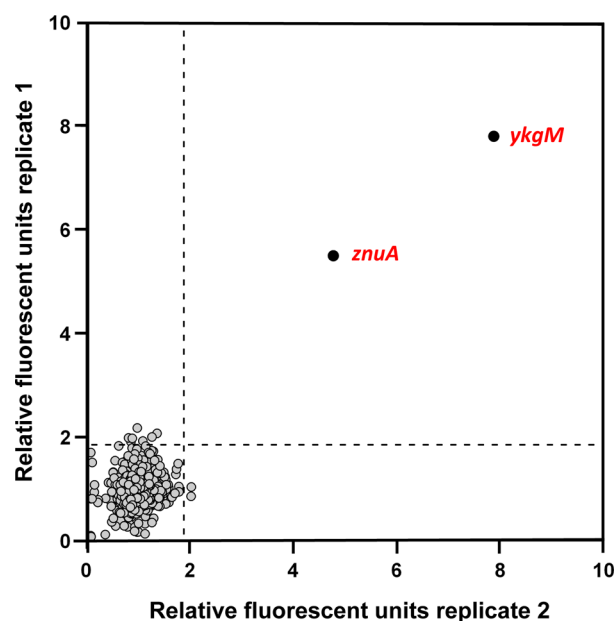


Figure 2. Replicate plot of *gfp*-promoter library screened against a subinhibitory concentration of compound SIT-ZS. Dashed lines represent 3 σ above the average relative fluorescent units of all strains.

ykgM and *znuA* promoter induction was the result of our proposed role for SIT-ZS in perturbing bacterial zinc homeostasis, we assayed all analogues against the *ykgM* and *znuA* *gfp*-promoter strains. In particular, we aimed to verify that the respective promoters were not simply sensitive to any compound with a spiro-indoline-thiadiazole backbone, such as compounds SIT-1 and SIT-2, which are known to be primarily involved in disrupting bacterial iron homeostasis. We observed that induction of both of the *ykgM* and *znuA* *gfp*-promoter strains occurred in the presence of each Z-series analogue; in contrast, however, none of the non-Z-series of compounds led to increased expression of either of the respective *gfp*-promoter strains (Figure 3). Thus, only those analogues showing zinc-specific suppression of toxicity were found to activate promoters involved in responding to zinc limitation, further

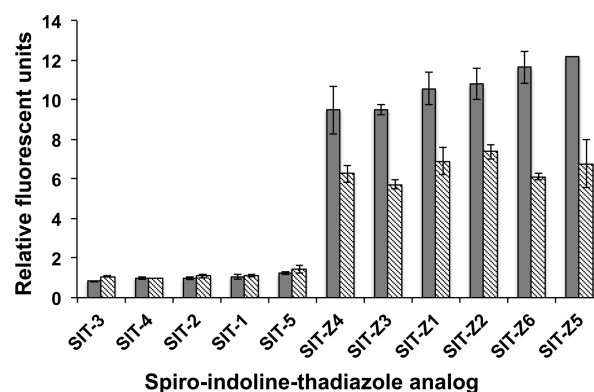


Figure 3. Perturbation of bacterial zinc homeostasis is specific to the Z-series of analogues. Individual strains of *gfp*-promoter strains, *ykgM* (gray bars) and *znuA* (hatched bars), grown in Chelex 100-treated minimal media were perturbed with a fourth of the concentration of the various analogues required for bacterial growth inhibition, where activation of the promoter strains was monitored via fluorescence. Bar graphs represent the mean \pm SD for three samples.

reinforcing the conclusion that the Z-series of compounds were involved in perturbing bacterial zinc homeostasis.

Compound SIT-Z5 Potentiates Carbapenem Activity against an NDM-1-Positive Strain of *K. pneumoniae*. Next, we endeavored to determine whether SIT-Z5 might be capable of resensitizing a metallo- β -lactamase-producing strain of bacteria to carbapenem class antibiotics. Thus, we performed checkerboard assays of SIT-Z5 in combination with the carbapenem antibiotic, meropenem, against an NDM-1-harboring clinical isolate of *K. pneumoniae*. Synergy was evident in the signature staircase pattern of growth in the pairwise matrix of concentrations tested. When used in combination with SIT-Z5, meropenem activity against *K. pneumoniae* was potentiated, where the MIC of the antibiotic against *K. pneumoniae* decreased from >2 to 0.25 μ M (Figure 4a).

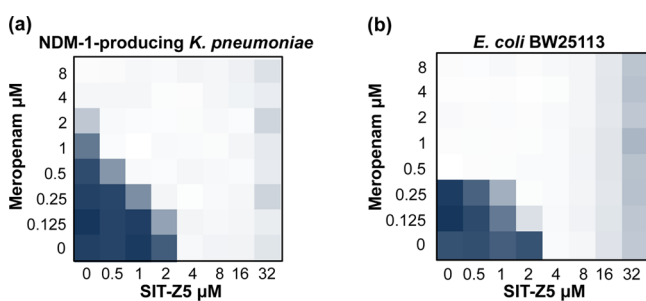


Figure 4. Potentiation of meropenem activity by SIT-Z5 is specific to bacteria harboring metallo- β -lactamase resistance. The effects of chemical–chemical interactions between meropenem and compound SIT-Z5 against (a) a carbapenem-resistant strain of *K. pneumoniae* and (b) a nonpathogenic laboratory strain of *E. coli* are represented by full bacterial growth (blue squares) to complete growth inhibition (white squares). Interactions are quantified by fractional inhibitory concentration (FIC) indices,³⁸ where values <0.5, 1, and >2 indicate compound synergy, additivity, and antagonism, respectively. The meropenem–SIT-Z5 profile against an NDM-1-harboring strain revealed a profoundly synergistic chemical–chemical interaction with an FIC index of 0.375. The compound pair against nonpathogenic *E. coli* yielded an additive response represented by an FIC index of 1.

To assess whether the observed potentiation of meropenem by SIT-Z5 was specific to the zinc-chelating properties of SIT-Z5, we assayed whether synergism between the compound pair could also be observed in the non-NDM-1-harboring bacterial strain, *E. coli* BW25113. Interestingly, we showed that, although profoundly synergistic against *K. pneumoniae*, the SIT-Z5–meropenem combination showed an additive antibacterial phenotype against *E. coli* (Figure 4b).

Next, we addressed whether synergy between SIT-Z5 and meropenem against *K. pneumoniae* was specific to carbapenem class compounds or whether SIT-Z5 was also capable of potentiating the action of additional antibiotics. We found that, although not as pronounced as when added in combination with meropenem, compound SIT-Z5 also potentiated the action of the carbapenem antibiotics imipenem, doripenem, and biapenem (Figure S2). However, such potentiation was not detected between SIT-Z5 and non-carbapenem β -lactams or non-cell-wall-active antibiotics.

Compound SIT-Z5 Demonstrates In Vitro Inhibition of NDM-1. We hypothesized that the mechanism of synergy between SIT-Z5 and meropenem was due to an inhibition of NDM-1 via zinc chelation by SIT-Z5 and a subsequent resumption of meropenem activity. To determine whether

SIT-Z5 was indeed capable of inhibiting NDM-1, dose–response assays were conducted in the absence of supplemental zinc, where SIT-Z5 was found to inhibit NDM-1 with an IC₅₀ value of 6.6 ± 1.3 μ M (Figure 5). At the concentration of SIT-Z5 tested, the MBL IMP-7 and serine- β -lactamase (SBL) TEM-1 were not significantly inhibited. The MBL VIM-2 showed a slight dose-dependent inhibition (~16%). SIT-Z5 was not soluble at higher concentrations and therefore could not be appropriately assayed for inhibition of VIM-2. These findings are consistent with reports in the literature in which the strength of zinc binding by the respective enzymes is in the order IMP > VIM > NDM.^{22–24} Collectively, these results are suggestive of preferential inhibition of NDM-1 by SIT-Z5; however, further study is required to substantiate this claim.

Analogues Specific to Zinc Perturbation Potentiate Meropenem Activity against an NDM-1-Positive Strain of *K. pneumoniae*. In addition to compound SIT-Z5, we wanted to determine whether those analogues with antibacterial activity that was specific to zinc perturbation—namely the Z-series of analogues—were capable of synergizing with meropenem against *K. pneumoniae*. With the exception of compound SIT-Z1, we observed synergy between meropenem and all zinc-specific perturbants when tested against *K. pneumoniae*, although we did not detect potentiation of meropenem activity when combined with any of the non-Z-series of analogues (Figure S3). With respect to the lack of synergy between SIT-Z1 and meropenem, a possible explanation for this may be the relatively low log *P* value displayed by the respective analogue as compared to all other compounds in the Z-series (Table 1). Specifically, it may be that SIT-Z1 is capable of infiltrating the outer membrane of *E. coli* K-12, but is unable to do so against *K. pneumoniae*.

Compound SIT-Z5 Is Synergistic with Meropenem against an NDM-1-Positive Strain of *K. pneumoniae* in a Mouse Model of Infection. In light of host toxicity concerns involving the therapeutic application of metal chelators, we sought to determine whether SIT-Z5 was capable of potentiating the action of meropenem in vivo at doses not associated with host toxicity, which was determined by examining weight loss and the body condition of mice. As such, we identified a preliminary dose of SIT-Z5 that was nontoxic to mice and then assessed the therapeutic potential of this concentration during infection. Specifically, mice were infected intraperitoneally with a sublethal dose of the clinical isolate, NDM-1-harboring *K. pneumoniae*. A single subcutaneous dose of drug was then administered 30 min post infection, and the effects of monotherapy and combination treatment of SIT-Z5 and meropenem on bacterial load in tissues was examined. Using a well-documented *K. pneumoniae* challenge model, we found that treatment with either SIT-Z5 or meropenem alone had no effect on bacterial burden; however, co-administration of the compounds resulted in a significant reduction of the bacterial load detected in the liver (Figure 6a) and spleen (Figure 6b).

DISCUSSION

The emergence of carbapenem-resistant Gram-negative pathogens in concert with the lean antibiotic development pipeline has resulted in a serious health crisis that will continue to worsen unless new therapeutic measures are soon met. Of particular concern are those strains of bacteria that, in addition to being recalcitrant to the action of carbapenems, also harbor resistance determinants to an array of additional antibiotics,

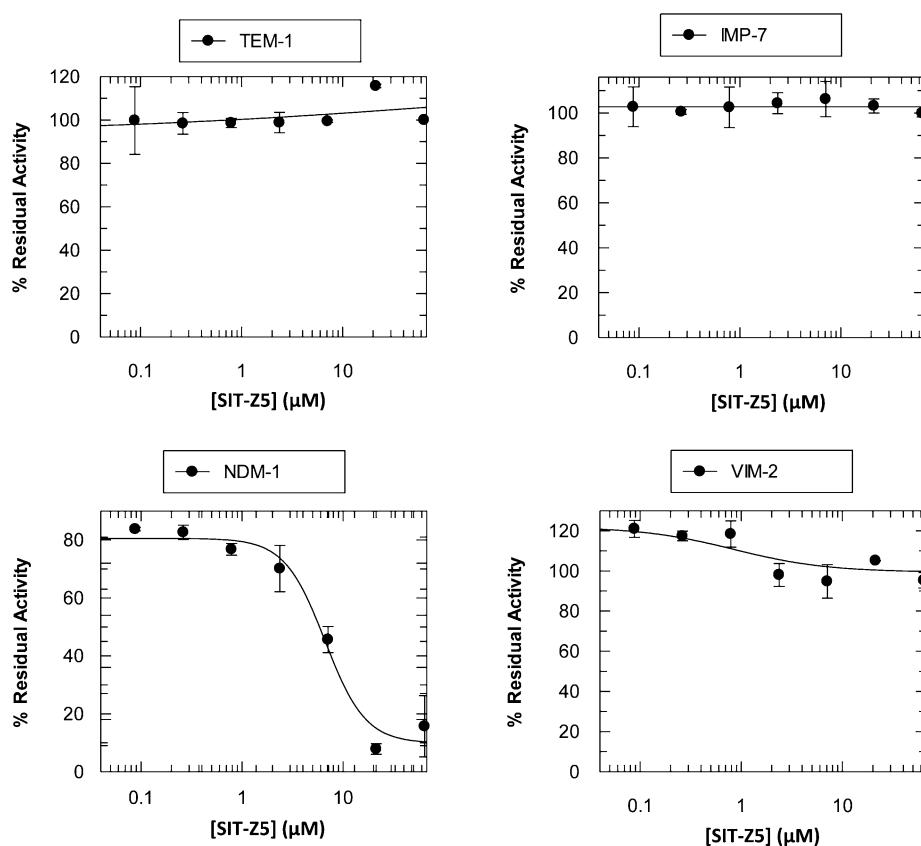


Figure 5. SIT-5Z shows dose-dependent inhibition of NDM-1 in vitro. SIT-5Z was assayed against purified enzyme as noted. NDM-1 showed dose-dependent inhibition with an observed IC_{50} value of $6.6 \pm 1.3 \mu\text{M}$. VIM-2 showed minimal inhibition, whereas IMP-7 and TEM-1 were unaffected by SIT-5Z. Error bars denote standard deviation of at least two technical replicates.

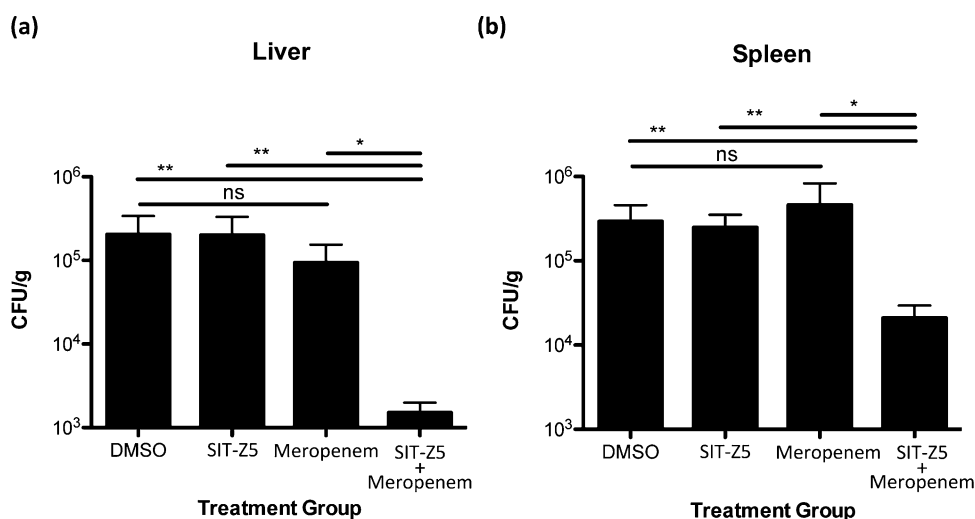


Figure 6. Compound SIT-5Z resensitizes NDM-1-containing *K. pneumoniae* to meropenem in vivo. CD1 mice were infected with 2×10^6 cfu *K. pneumoniae* ip. All groups of mice were treated with a subcutaneous injection of 10 mg/kg meropenem, 10 mg/kg SIT-5Z inhibitor, or a combination of both antibiotic and inhibitor. Control mice received diluting buffer. Mice were euthanized at 48 h post infection, and both the spleen and liver were harvested. Bacterial load of both the (a) liver and (b) spleen were determined. Data were pooled from three separate experiments ($n = 12$ per group). Significance was determined using a *t* test. (*) $p < 0.05$; (**) $p < 0.01$.

such as in the case of NDM-1-producing pathogens.⁷ Drug-resistant pathogenic Enterobacteriaceae have become a scourge to nosocomial environments, as their resilience to the current treatment strategies has afforded them the opportunity to proliferate. Furthermore, innate resistance offered by the Gram-negative outer membrane makes efforts to identify novel

antibacterial compounds exceedingly difficult. In this work we explored a series of chelator analogues having structures based on a spiro-indoline-thiadiazole chemical scaffold that we recently reported as being an intracellular inhibitor of *E. coli* growth through disruption of iron homeostasis via chelation.¹⁴ Given the susceptibility of Gram-negative bacteria to the

respective chemical series, we hypothesized that the bioactive scaffold would be a good starting point to investigate additional chelator analogues that, rather than iron, chelate and perturb bacterial zinc homeostasis. Zinc is required for the activity of metallo- β -lactamases; thus, we reasoned that a chelator whose antibacterial activity was due to zinc sequestration might synergize with carbapenem antibiotics and resensitize an otherwise antibiotic-resistant strain of Enterobacteriaceae to the action of carbapenems. Indeed, we report here the identification of a series of spiro-indoline-thiadiazole chelators capable of potentiating carbapenem activity against a clinical isolate of NDM-1-harboring *K. pneumoniae*. Furthermore, we demonstrate in vivo that one such analogue shows promise as a nontoxic chelator that resensitizes a metallo- β -lactamase pathogen to the action of meropenem. We present compelling evidence that the mechanism of action of these respective compounds is via their ability to chelate and limit bacterial zinc availability.

Chelators are generally known to be nonspecific and capable of forming complexes with various metal species.²⁵ Indeed, such promiscuity with respect to metal binding is among the most prominent features of chelators limiting their therapeutic use. However, there are many features that contribute to the governing principles of metal–ligand coordination chemistry, including shape, solubility, lipophilicity, and kinetics—all of which affect the biological outcome of a chelator–chelate relationship.¹⁰ Therefore, we reasoned that even subtle modifications to the spiro-indoline-thiadiazole ligand skeleton could influence the behavior of a given analogue when introduced to the cellular environment.

Having previously established that compound **SIT-1** was specific to perturbing iron homeostasis,¹⁴ we began by exploring the zinc versus iron specificity of this compound and analogues thereof. In exploring a range of chemical modifications at the R1 positions we found that, for each of the analogues tested, the presence of a moiety bonded to the R1 carbon alone resulted in a zinc-specific activity suppression profile. This suggested that a common characteristic—such as lipophilicity, ligand/metal stoichiometry, or coordination geometry of the metal–chelate complex—determined by the R1 moiety affected zinc-specific suppression of antibacterial activity. In the first instance, lipophilicity is a salient chemical feature that is known to correlate with compound toxicity,²⁶ a characteristic that we observed to be consistent in the case of our analogues. Because all modifications at the R1 position of the **Z**-series of compounds are carbon-based substituents, we considered whether lipophilicity also contributed to the observed metal suppression profiles. However, we found no correlation between lipophilicity and zinc-specific perturbation by the analogues. Structural studies between Fe^{2+} and Zn^{2+} , and each **SIT-1** and **SIT-Z5**, similarly indicated that neither was stoichiometry responsible for the zinc specificity exhibited by **SIT-Z5**, because the same 2:1 ligand/metal stoichiometry was observed for each complex. However, insight was gleaned from the coordination geometries of the various ligand–metal complexes because, rather than an octahedral geometry that was indicated for the **SIT-1**– Fe^{2+} , **SIT-1**– Zn^{2+} , and **SIT-Z5**– Fe^{2+} complexes, the predicted conformation of the **SIT-Z5**– Zn^{2+} complex was tetrahedral. Such findings raise the possibility that **SIT-Z5** and, potentially, all analogues within the **Z**-series are more stable in the open merocyanine form when coordinated with Zn^{2+} in a tetrahedral rather than an octahedral geometry. Alternatively, the observed Zn^{2+} specificity conferred by the **Z**-series of

compounds may be due to the localization of such molecules within the bacterial cell. Indeed, this study has revealed a chemical trend whereby phenyl-spiro-indoline-thiadiazole compounds with substitutions exclusively at the R1 position are capable of undergoing zinc-specific suppression of antibacterial activity. Interestingly, the zinc specificity displayed by the respective **Z**-series of molecules is corroborated by our results from both *gfp*-promoter experiments and chemical–chemical interaction assays with *K. pneumoniae*. Screening a *gfp*-promoter–reporter genomic collection revealed that, of the approximately 2000 *E. coli* promoters, only *znuA* and *ykgM* were induced by **SIT-Z5**. Both of these genes are known to be up-regulated in response to zinc limitation.^{18,20,21} Indeed, such observations are consistent with those of a previous study that investigated the transcriptional response of *E. coli* to the intracellular zinc chelator *N,N,N',N'*-tetrakis(2-pyridylmethyl)ethylenediamine (TPEN).²⁷ In the respective study, the only zinc-related transcripts to be identified were *ykgM*, *zinT* (formerly *yodA*), *znuA*, and *znuC*. We are unable to address whether we would have identified increased activation of the promoter for *zinT* as a promoter–GFP construct for the respective gene is absent from the *gfp*-promoter–reporter genomic library. In the case of *znuC*, the discrepancy between its increased transcriptional response to TPEN and our inability to identify promoter activation of the gene is less clear. *ZnuA* and *ZnuC* are members of the same multiprotein zinc transporter, where *ZnuA* serves as the periplasmic zinc binding protein and *ZnuC* binds to ATP.^{18,28} It is possible that the direct interaction between zinc and *ZnuA* results in greater transcriptional sensitivity of *znuA* versus *znuC* when faced with a zinc replete environment; however, such an explanation is purely speculative. Nonetheless, we confirmed specificity of activation of *ykgM* and *znuA* by demonstrating that the activity of these promoter–reporter strains was unaffected by the non-**Z**-series, but was induced by all **Z**-series of analogues. Additionally, it was striking to us that, with the exception of **SIT-Z1**, our observation of zinc specificity against *E. coli* regarding the **Z**-series of analogues correlated with the in vitro potentiation of meropenem against NDM-1-producing *K. pneumoniae*. Collectively, the results of these experiments suggest a distinct mechanism of action by the respective compound series against the bacterial cell. In turn, we argue that specifically the **Z**-series of compounds disturb bacterial zinc homeostasis via chelation and limitation of the metal and that such perturbation is their primary, if not exclusive, antibacterial mechanism of action.

In addition to establishing the **Z**-series of compounds as perturbants of bacterial zinc homeostasis, the work herein also revealed an important and potentially therapeutic application for these molecules as adjuvants for the treatment of infections caused by carbapenem-resistant bacterial pathogens. By demonstrating the in vitro inhibition of NDM-1 by **SIT-Z5**, coupled with our in vivo observations that a nontoxic dose of **SIT-Z5** was effective at resensitizing an NDM-1-producing strain of *K. pneumoniae* to meropenem activity, this work positions **SIT-Z5** as a promising candidate in the treatment of metallo- β -lactamase-producing bacterial infections.

The use of chelators in medicine is often approached with trepidation given their complicated drug safety profiles and the many significant side effects associated with their use.^{29–31} However, this has not prevented the long-standing use of chelators as therapeutic agents against iron overload disease,^{32,33} nor have discussion and research been thwarted regarding the

development of new chelators for the treatment of various neurodegenerative diseases^{13,34,35} and certain types of cancer.³⁶ Thus, there exists a strong precedent for both current and potential future uses of chelators as pharmaceuticals, which we argue should be considered by both researchers and medical practitioners within the field of infectious disease. Evaluating the long-term effects of a short therapeutic course of SIT-Z5 is a necessary step toward a potential clinical future for the respective chelator; however, our preliminary findings that SIT-Z5 exhibits synergism with meropenem at a concentration that is not overtly toxic to mice is highly encouraging.

NDM-1-harboring *K. pneumoniae* is among the most dreaded and difficult-to-treat strains of pathogenic bacteria currently plaguing the medical community. Due to the obstinacy of the outer membrane, identifying new antibacterial small molecules capable of infiltrating the respective barrier has proved exceedingly challenging. Thus, rather than continuing with the traditional antibiotic drug discovery regiment—which is to conduct chemical screens to identify new antibacterial small molecules that target a single mechanism—an alternative strategy is to develop compounds that serve as adjuvants to current antibiotics. The difficulty in achieving single-metal targeting by a given chelator, coupled with grave toxicity concerns during unsuccessful therapeutic attempts using EDTA for the treatment of various maladies, has incited staunch misgivings about the application of chelators in medicine.¹⁰ However, the relationship between each chelator and its chelate is highly unique such that, when applied to a system as complex as the cell, the biological outcomes, including the degree of host toxicity, can be vastly different. In the work herein we present a series of spiro-indoline-thiadiazole compounds that, through chelation of zinc, compromise the mechanism of metallo- β -lactamase antibiotic resistance, thereby potentiating the activity of carbapenem antibiotics and, in turn, reinstating efficacy of the drug class against NDM-1-harboring *K. pneumoniae*.

MATERIALS AND METHODS

Bacterial Strains, Growth Media, and Reagents. *E. coli* K-12 strain BW25113 was used for all experiments with the exception of those strains contained in the *gfp*-promoter library, where the background strain for the collection is *E. coli* MG1655, and experiments involving the *K. pneumoniae* clinical isolate. The *gfp*-promoter library was a kind gift from Uri Alon and Michael Surette, and the *K. pneumoniae* strain was gifted from Michael Mulvey to Gerard D. Wright. All growth experiments were conducted in liquid media under aerobic conditions in Chelex 100 resin (Bio-Rad)-treated M9 minimal media. Minimal medium was composed of 1 \times M9 minimal salts prepared from 5 \times M9 minimal salts stock (Sigma-Aldrich), 0.2% v/v Casamino acids (BD Biosciences), 10 μ M of each aromatic amino acid, L-tyrosine, L-tryptophan, and L-phenylalanine, 1 μ M thiamin, and 0.4% v/v glucose. Unless stated otherwise, all reagents and chemicals, including the metal salts ferrous chloride and zinc chloride, were purchased from Sigma-Aldrich. Compounds SIT-1, SIT-2, SIT-3, SIT-4 and SIT-Z5 were purchased from ChemBridge and dissolved in DMSO. Compounds SIT-5, SIT-Z1, SIT-Z2, SIT-Z3, SIT-Z4, and SIT-Z6 were synthesized (see the Supporting Information).

Minimum Inhibitory Concentration Determinations. All bacterial strains were grown overnight at 37 °C with shaking at 250 rpm in 5 mL of M9 minimal medium. Saturated cultures were subsequently diluted 1:100 into M9 minimal media and grown to an OD_{600 nm} of 0.2 for growth in Chelex 100 resin-treated

M9 minimal medium. Bacteria were again diluted 1:100,000 into Chelex 100 resin-treated M9 minimal medium containing the final concentration of compound to be tested. Bacteria with compound were incubated under stationary conditions at 37 °C, and growth at OD_{600 nm} was measured after 18 h unless stated otherwise.

Screening Analogues against *E. coli* K-12 *gfp*-Promoter Library. Strains from the *gfp*-promoter genomic library arrayed in 96-well plates were inoculated from frozen stocks into fresh M9 minimal medium containing 25 μ g mL⁻¹ kanamycin using the Duetz cryoreplicator.³⁷ Inoculated plates were shaken for 18 h at 37 °C and 200 rpm to achieve saturated cultures. Strains were then subcultured at a 1:100 dilution by transferring 2 μ L of culture into 198 μ L of M9 minimal medium containing 25 μ g mL⁻¹ kanamycin and returned to shaking at 37 °C and 250 rpm until bacteria reached an OD_{600 nm} of 0.2. Strains were then diluted 1:200 in Chelex resin-treated M9 minimal medium with 25 μ g mL⁻¹ kanamycin, and samples were either treated with one-fourth of the minimum inhibitory concentration of analogue of interest or grown in Chelex resin-treated M9 minimal medium alone. Bacteria were incubated at 37 °C for 16 h, and growth was measured and recorded at OD_{600 nm}. Screening SIT-Z5 against the complete genomic library was performed in duplicate; for all other analogues against *znuA* and *ykgM* promoter strains, assays were conducted in triplicate.

Metal Suppression Experiments. *E. coli* BW25113 was treated as described above for MIC experiments; however, rather than testing the final 1:100,000 dilution of bacteria against a range of compound concentrations, here we added bacteria to double the previously established MIC of our compound of interest, combined with an equimolar concentration of either zinc chloride or iron chloride. Samples were then incubated under stationary conditions at 37 °C, and bacterial growth was measured at OD_{600 nm} after 18 h. Results are represented as the mean \pm SD for three samples.

Crystallization Conditions and Crystal Structure Determination. Maroon crystals of the SIT-Z5–Zn²⁺ and SIT-Z5–Fe²⁺ complexes were each generated by slow evaporation at ambient temperature of a 1:1 (v/v) methanol/chloroform solution containing 1:1.2 (molar ratio) of SIT-Z5 powder and either ferrous chloride or zinc chloride. Crystals of both SIT-Z5–Zn²⁺ and SIT-Z5–Fe²⁺ were observed after 3 weeks, and single-crystal X-ray crystallographic analyses were conducted. Diffraction data for SIT-Z5–Zn²⁺ were obtained using ω -scans via a Bruker SMART6000 CCD area detector mounted on a fixed- χ three-circle D8 goniometer using a Rigaku Cu rotating anode with cross-coupled mirrors and Cu K α radiation ($\lambda = 1.54178$ Å). SIT-Z5–Fe²⁺ data were collected on the Bruker Smart Apex2 CCD instrument with a Mo sealed tube source and a curved graphite monochromator (Mo K α radiation ($\lambda = 0.71073$ Å)). Data refinement was accomplished using SHELXL (Sheldrick, refinement).

Chemical–Chemical Interaction Assays. For each assay an 8 \times 8 matrix was prepared at the appropriate drug concentration. Bacterial strains were grown for 18 h at 37 °C with shaking at 250 rpm in 5 mL of M9 minimal medium. Saturated cultures were subsequently diluted 1:100 into M9 minimal medium and grown to an OD_{600 nm} of 0.2. Bacteria were again diluted 1:100,000 into Chelex 100 resin-treated M9 minimal medium and added to the compound assay plate. Plates were then incubated under stationary conditions at 37 °C, where growth at OD_{600 nm} was measured after 18 h unless stated otherwise. Assays for each compound combination were

performed in duplicate, and averaged values were used to calculate the FIC index.

Dose–Response Enzyme Assays. Enzyme (final concentrations: NDM-1, 50 nM; IMP-7, 10 nM; VIM-2, 20 nM; TEM-1, 1 nM) was incubated with **SIT-5Z** in serial 1:3 dilutions from 64 μ M for 10 min. The buffer used was Chelex-treated 50 mM HEPES (pH 7.5) with 0.01% Tween-20. Inhibitor was diluted in DMSO and added for a final [DMSO] of 2.5%. Addition of substrate (nitrocefin, final concentration = 20 μ M) initiated reaction. Progress curves of hydrolysis at 37 °C were monitored at 490 nm in 96-well microplate format using a Spectramax reader (Molecular Devices).

Mice. All animals were housed in a specific pathogen-free unit in the Central Animal Facility at McMaster University. All experimental protocols were approved by, and performed in accordance with, the McMaster Animal Research Ethics Board. Female 5–7-week-old CD1 mice were purchased from Charles River.

Bacterial Infections. For all organ bacterial load experiments, mice were infected intraperitoneally (ip) with a dose of 2×10^6 colony-forming units (cfu) of *K. pneumoniae*. Mice were then euthanized 48 h post infection, and the spleen and liver were harvested. Organs were placed into 1 mL of sterile PBS on ice and then homogenized (Mixer Mill 400; Retsch). Organ homogenates were then serially diluted in PBS and plated on Brilliant Green agar (BD Biosciences) for cfu enumeration. For all experiments, mice were treated 30 min post infection with a specified subcutaneous dose of either diluting buffer, meropenem, **SIT-Z5** inhibitor, or a combination of both antibiotic and inhibitor. Diluting buffer consisted of water/ethanol/PEG-400 in a ratio of 1:1:1.6, respectively. DMSO was the vehicle solvent for both meropenem and **SIT-Z5**, which was added to the diluting buffer at 7.1%.

■ ASSOCIATED CONTENT

■ Supporting Information

The Supporting Information is available free of charge on the ACS Publications website at DOI: 10.1021/acsinfecdis.5b00033.

Figures S1–S3 display a crystal structure of the **SIT-Z5**– Fe^{2+} coordination complex, chemical–chemical interaction assays between **SIT-Z5** and various antibiotics, and chemical–chemical interaction assays between meropenem and various **SIT** analogues; supplementary Materials and Methods describe chemical synthesis of the analogues (PDF)

■ AUTHOR INFORMATION

Corresponding Author

*(E.D.B.) E-mail: ebrown@mcmaster.ca.

Author Contributions

S.B.F. and E.D.B. designed the study; S.A.R. performed animal experiments; A.M.K. performed in vitro NDM-1 inhibition assays; S.S.G. synthesized analogues; W.W. obtained crystals, and J.F.B. performed diffraction analysis; S.B.F. performed all other experiments and analyzed data; S.B.F. and E.D.B. wrote the manuscript. All authors reviewed and approved the final report.

Funding

This work was supported by an operating grant from the Canadian Institutes of Health Research (CIHR; MOP-81330) and salary awards from the Canada Research Chairs program to E.D.B., G.D.W., and B.K.C.

Notes

The authors declare no competing financial interest.

■ REFERENCES

- (1) Nordmann, P., Poirel, L., Walsh, T. R., and Livermore, D. M. (2011) The emerging NDM carbapenemases. *Trends Microbiol.* 19, 588–595.
- (2) Kumarasamy, K. K., Toleman, M. A., Walsh, T. R., Bagaria, J., Butt, F., Balakrishnan, R., Chaudhary, U., Doumith, M., Giske, C. G., Irfan, S., Krishnan, P., Kumar, A. V., Maharjan, S., Mushtaq, S., Noorie, T., Paterson, D. L., Pearson, A., Perry, C., Pike, R., Rao, B., Ray, U., Sarma, J. B., Sharma, M., Sheridan, E., Thirunaryan, M. A., Turton, J., Upadhyay, S., Warner, M., Welfare, W., Livermore, D. M., and Woodford, N. (2010) Emergence of a new antibiotic resistance mechanism in India, Pakistan, and the UK: a molecular, biological, and epidemiological study. *Lancet Infect. Dis.* 10, 597–602.
- (3) Nordmann, P., Dortet, L., and Poirel, L. (2012) Carbapenem resistance in Enterobacteriaceae: here is the storm! *Trends Mol. Med.* 18, 263–272.
- (4) Cornaglia, G., Giamarellou, H., and Rossolini, G. M. (2011) Metallo- β -lactamases: a last frontier for β -lactams? *Lancet Infect. Dis.* 11, 381–393.
- (5) Worthington, R. J., Bunders, C. A., Reed, C. S., and Melander, C. (2012) Small molecule suppression of carbapenem resistance in NDM-1 producing *Klebsiella pneumoniae*. *ACS Med. Chem. Lett.* 3, 357–361.
- (6) Drawz, S. M., Papp-Wallace, K. M., and Bonomo, R. A. (2014) New β -lactamase inhibitors: a therapeutic renaissance in an MDR world. *Antimicrob. Agents Chemother.* 58, 1835–1846.
- (7) Laxminarayan, R., Duse, A., Watal, C., Zaidi, A. K. M., Wertheim, H. F. L., Sumpradit, N., Vlieghe, E., Hara, G. L., Gould, I. M., Goossens, H., Greko, C., So, A. D., Bigdeli, M., Tomson, G., Woodhouse, W., Ombaka, E., Peralta, A. Q., Qamar, F. N., Mir, F., Kariuki, S., Bhutta, Z. A., Coates, A., Bergstrom, R., Wright, G. D., Brown, E. D., and Cars, O. (2013) Antibiotic resistance—the need for global solutions. *Lancet Infect. Dis.* 13, 1057–1098.
- (8) Shlaes, D. M. (2013) New β -lactam- β -lactamase inhibitor combinations in clinical development. *Ann. N. Y. Acad. Sci.* 1277, 105–114.
- (9) King, A. M., Reid-Yu, S. A., Wang, W., King, D. T., De Pascale, G., Strynadka, N. C., Walsh, T. R., Coombes, B. K., and Wright, G. D. (2014) Aspergillomarasmine A overcomes metallo- β -lactamase antibiotic resistance. *Nature* 510, 503–506.
- (10) Franz, K. J. (2013) Clawing back: broadening the notion of metal chelators in medicine. *Curr. Opin. Chem. Biol.* 17, 143–149.
- (11) Whitnall, M., Howard, J., Ponka, P., and Richardson, D. R. (2006) A class of iron chelators with a wide spectrum of potent antitumor activity that overcomes resistance to chemotherapeutics. *Proc. Natl. Acad. Sci. U. S. A.* 103, 14901–14906.
- (12) Jacobsen, J. A., Fullagar, J. L., Miller, M. T., and Cohen, S. M. (2011) Identifying chelators for metalloprotein inhibitors using a fragment-based approach. *J. Med. Chem.* 54, 591–602.
- (13) Perez, L. R., and Franz, K. J. (2010) Minding metals: tailoring multifunctional chelating agents for neurodegenerative disease. *Dalton Trans.* 39, 2177–2187.
- (14) Falconer, S. B., Wang, W., Gehrke, S. S., Cuneo, J. D., Britten, J. F., Wright, G. D., and Brown, E. D. (2014) Metal-induced isomerization yields an intracellular chelator that disrupts bacterial iron homeostasis. *Chem. Biol.* 21, 136–145.
- (15) Finney, L. A., and O'Halloran, T. V. (2003) Transition metal speciation in the cell: insights from the chemistry of metal ion receptors. *Science* 300, 931–936.
- (16) Outten, C. E., and O'Halloran, T. V. (2001) Femtomolar sensitivity of metalloregulatory proteins controlling zinc homeostasis. *Science* 292, 2488–2492.
- (17) Zaslaver, A., Bren, A., Ronen, M., Itzkovitz, S., Kikoin, I., Shavit, S., Liebermeister, W., Surette, M. G., and Alon, U. (2006) A comprehensive library of fluorescent transcriptional reporters for *Escherichia coli*. *Nat. Methods* 3, 623–628.

- (18) Patzer, S. I., and Hantke, K. (1998) The ZnuABC high-affinity zinc uptake system and its regulator Zur in *Escherichia coli*. *Mol. Microbiol.* 28, 1199–1210.
- (19) Makarova, K. S., Ponomarev, V. A., and Koonin, E. V. (2001) Two C or not two C: recurrent disruption of Zn-ribbons, gene duplication, lineage-specific gene loss, and horizontal gene transfer in evolution of bacterial ribosomal proteins. *Genome Biol.* 2 (9), No. research0033.
- (20) Graham, A. I., Hunt, S., Stokes, S. L., Bramall, N., Bunch, J., Cox, A. G., McLeod, C. W., and Poole, R. K. (2009) Severe zinc depletion of *Escherichia coli*: roles for high affinity zinc binding by ZinT, zinc transport and zinc-independent proteins. *J. Biol. Chem.* 284, 18377–18389.
- (21) Hensley, M. P., Gunasekera, T. S., Easton, J. A., Sigdel, T. K., Sugarbaker, S. A., Klingbeil, L., Breece, R. M., Tierney, D. L., and Crowder, M. W. (2012) Characterization of Zn(II)-responsive ribosomal proteins YkgM and L31 in *E. coli*. *J. Inorg. Biochem.* 111, 164–172.
- (22) Laraki, N., Franceschini, N., Rossolini, G. M., Santucci, P., Meunier, C., de Pauw, E., Amicosante, G., Frère, J. M., and Galleni, M. (1999) Biochemical characterization of the *Pseudomonas aeruginosa* 101/1477 metallo- β -lactamase IMP-1 produced by *Escherichia coli*. *Antimicrob. Agents Chemother.* 43, 902–906.
- (23) Docquier, J. D., Lamotte-Brasseur, J., Galleni, M., Amicosante, G., Frère, J. M., and Rossolini, G. M. (2003) On functional and structural heterogeneity of VIM-type metallo- β -lactamases. *J. Antimicrob. Chemother.* 51, 257–266.
- (24) Thomas, P. W., Zheng, M., Wu, S., Guo, H., Liu, D., Xu, D., and Fast, W. (2011) Characterization of purified New Delhi metallo- β -lactamase-1. *Biochemistry* 50, 10102–10113.
- (25) Hider, R. C. (2002) Design of therapeutic chelating agents. *Biochem. Soc. Trans.* 30, 751–754.
- (26) Leeson, P. D., and Springthorpe, B. (2007) The influence of drug-like concepts on decision-making in medicinal chemistry. *Nat. Rev. Drug Discovery* 6, 881–890.
- (27) Sigdel, T. K., Easton, J. A., and Crowder, M. W. (2006) Transcriptional response of *Escherichia coli* to TPEN. *J. Bacteriol.* 188, 6709–6713.
- (28) Yatsunyk, L. A., Easton, J. A., Kim, L. R., Sugarbaker, S. A., Bennett, B., Breece, R. M., Vorontsov, I. I., Tierney, D. L., Crowder, M. W., and Rosenzweig, A. C. (2008) Structure and metal binding properties of ZnuA, a periplasmic zinc transporter from *Escherichia coli*. *J. Biol. Inorg. Chem.* 13, 271–288.
- (29) Drosos, A. A., Geogiou, P., Politi, E. N., and Voulgari, P. V. (1997) D-Penicillamine in early rheumatoid arthritis. *Clin. Exp. Rheumatol.* 15, 580–581.
- (30) Brown, M. J., Willis, T., Omalu, B., and Leiker, R. (2006) Deaths resulting from hypocalcemia after administration of edetate disodium: 2003–2005. *Pediatrics* 118, e534–e536.
- (31) Gattermann, N., Finelli, C., Porta, M. D., and Fenau, P. (2010) Deferasirox in iron-overloaded patients with transfusion-dependent myelodysplastic syndromes: results from the large 1-year EPIC study. *Leuk. Res.* 34, 1143.
- (32) Olivieri, N. F., and Brittenham, G. M. (1997) Iron-chelating therapy and the treatment of thalassemia. *Blood* 89, 739–761.
- (33) Olivieri, N. F. (1999) The β -thalassemias. *N. Engl. J. Med.* 341, 99–109.
- (34) Li, X., Jankovic, J., and Le, W. (2011) Iron chelation and neuroprotection in neurodegenerative diseases. *J. Neural Transm* 118, 473–477.
- (35) Hider, R. C., Roy, S., Ma, Y. M., Le Kong, X., and Preston, J. (2011) The potential application of iron chelators for the treatment of neurodegenerative diseases. *Metallomics* 3, 239–249.
- (36) Torti, S. V., and Torti, F. M. (2013) Iron and cancer: more ore to be mined. *Nat. Rev. Cancer* 13, 342–355.
- (37) Duetz, W. A., Rüedi, L., Hermann, R., O'Connor, K., Büchs, J., and Witholt, B. (2000) Methods for intense aeration, growth, storage, and replication of bacterial strains in microtiter plates. *Appl. Environ. Microbiol.* 66, 2641–2646.
- (38) Pillai, S. K., Moellering, R. C., and Eliopoulos, G. M. (2005) Antimicrobial combinations. In *Antibiotics in Laboratory Medicine*, 5th ed., pp 365–440, Lippincott Williams and Wilkins, Philadelphia, PA, USA.
- (39) Holmberg, B. (1944) Benzoyl- and thiobenzoylthioglycolic acids and thiobenzohydrazide. *Ark. Kemi, Mineral. Geol. Ser. A* 17, 23.
- (40) Singh, N. K., Singh, S. B., and Shrivastav, A. (2002) Antitumour and immunomodulatory effects of Cu(II) complexes of thiobenzoylthiohydrazide. *Met Based Drugs* 9, 109–118.
- (41) Shome, S. C., Gangopadhyay, P. K., and Gangopadhyay, S. (1976) Extraction and spectrophotometric determination of ruthenium and osmium with thiobenzoylthiohydrazide. *Talanta* 23, 603–605.